Penerbit Akademia Baru

Journal of Advanced Research Design

Journal homepage:
https://akademiabaru.com/submit/index.php/ard
ISSN: 2289-7984

Diagnosis of Skin Melanoma Utilizing an Advanced Combination of Improved Meta-GVF Algorithms

Zaid Sadiq Naama[1], Safa Sami Abdul-Jabbar[1,*], Amer Almahdawi[1], El-Sayed M. El-kenawy[2,3]

[1] Computer Science Department, College of Science for Women, University of Baghdad, Baghdad, Iraq
[2] School of ICT, Faculty of Engineering, Design and Information & Communications Technology (EDICT), Bahrain Polytechnic, PO Box 33349, Isa Town, Bahrain
[3] Applied Science Research Centre, Applied Science Private University, Amman, Jordan

ARTICLE INFO

Article history:
Received 24 February 2025
Received in revised form 7 March 2025
Accepted 15 July 2025
Available online 28 July 2025

Keywords:
Melanoma; early detection; machine learning; diagnostic systems; meta-GVF algorithms

ABSTRACT

The rising global prevalence of skin cancer has become a significant public health concern. Although melanoma accounts for only about 1% of all skin cancer cases, it is responsible for the majority of skin cancer-related deaths. Early detection is critical, as it can raise the five-year survival rate to over 90%. However, the prognosis for metastatic melanoma remains poor, with a five-year survival rate of only 10–15%. Computer-aided diagnostic systems, utilizing machine learning and deep learning models, have shown promising results in analysing skin lesions and detecting melanoma. Despite these advancements, diagnostic accuracy is still limited by challenges such as the lack of distinct colour variation in skin lesions and the absence of reliable methods for assessing melanoma thickness—a crucial factor for prognosis and treatment planning. This study introduces an innovative approach to diagnosing skin melanoma using an advanced Meta-GVF algorithm, achieving an accuracy of 85.5%. The main finding is that, through shape modelling and well-chosen initial conditions, the contour can effectively move toward the correct boundary. Additionally, with further development, boundary detection techniques could help automate the initialization process in Meta-GVF, enabling the automated diagnosis of skin abnormalities.

1. Introduction

The purpose of this research was to further develop an automated computerized system for diagnosing skin melanoma, with a strong focus on creating algorithms that can effectively utilize information and image data obtained from various medical imaging techniques [1-3]. These algorithms aim to assist dermatologists in diagnosing skin lesions. With access to a large database of skin images featuring diverse diagnoses through the ISDIS, there is significant potential for this diagnostic system to make substantial contributions to skin cancer detection. This advancement could help reduce the diagnostic burden on dermatologists and decrease the number of unnecessary biopsies and surgeries [4-6].

* *Corresponding author*
E-mail address: safa.s@csw.uobaghdad.edu.iq

https://doi.org/10.37934/ard.140.1.8395

Melanoma is a form of skin cancer that originates in melanocytes, the cells responsible for producing skin pigments. Although melanoma accounts for 75% of all skin cancer-related deaths, it is almost 100% curable if recognized and treated early. Given the rising incidence of melanoma and increasing healthcare costs, developing computerized systems for melanoma diagnosis has become a major focus of research. Recently, two Meta-GVF algorithms have been implemented to classify one of four types of skin lesions and isolate melanoma [7]. The first algorithm assumes closed circular lesions, while the second is capable of segmenting any irregular lesion. This research builds on previous work with these algorithms by optimizing them to detect lesions of any shape and accurately delineate their borders [8].

1.1 Background

The term melanoma is derived from the Greek words melas, meaning black and -oma, meaning tumour. Melanoma is a malignant tumour of melanocytes. Both genetic and environmental factors contribute to the aetiology of melanoma. The incidence of melanoma has steadily increased, with an estimated 59,695 deaths worldwide in 2008. This number has risen since the 1990s, highlighting the need for widespread education on early detection techniques and the promotion of self-skin examination among the general population. Survival rates are strongly correlated with the thickness of a melanoma at the time of diagnosis. Patients with thin melanomas (≤1 mm) have a 94-98% 5-year survival rate, while those with thick melanomas (>4 mm) have a 15-40% survival rate [9,10]. Survival rates drastically decrease once the disease becomes invasive and metastatic [11,12].

Therefore, it is critical to routinely screen for early-stage melanoma to increase detection rates. Clinical examination is useful for identifying large, irregular or elevated melanocytic lesions, but it is less effective for detecting small, flat or colour-variegated lesions. Accurate diagnosis is essential to avoid unnecessary morbidity [13]. Dermoscopy, a non-invasive technique, allows the evaluation of colours and microstructures not visible to the naked eye. However, studies have shown that the sensitivity and specificity of diagnosing melanoma through dermoscopy remain relatively low. To improve early detection rates, automated image analysis methods have been developed. This paper describes a new method for segmenting and isolating skin lesions, which has shown potential in melanoma treatment by utilizing region-based active contours [14], as detailed in Table 1.

Table 1
Previous studies

Reference Number	Study Focus	Key Findings or Context
[9,10]	Survival rates based on melanoma thickness	Patients with thin melanomas (≤1 mm) have a 94-98% 5-year survival rate; thick melanomas (>4 mm) have a 40-15% survival rate.
[11,12]	Progression of melanoma	The survival rate drastically decreases with invasive and metastatic disease.
[13]	Clinical examination of melanoma	Clinical examination is useful for large, irregular lesions but less effective for small, flat or colour-variegated lesions.
[14]	New method of lesion analysis	A new method of segmenting and isolating skin lesions potentially indicative of melanoma using region-based active contour.

1.2 Purpose

The principal feature of Gradient Vector Flow Active Contours (GVFACs) is the replacement of the traditional external force with a more accurate and reliable force derived from the gradient vectors of a smoothed and slightly diffused version of the image [15]. This approach involves minimizing an

energy functional derived from the image, which serves as another zero-level set function. The optimal solution is the creation of Meta-Forms, which are analogous to the object but possess the correct topological configuration, acting as a singular global minimum of the energy functional. The curve then evolves by applying a flow function h(x,y,t) to deform the Meta-Form as closely as possible to the object [16]. This process is driven by another energy function, with the force being the gradient vector field of h. This phase of GVFACs has been successfully implemented in the segmentation of melanoma lesions, though it has certain limitations.

GVFACs aim to overcome a significant drawback of traditional active contour models: their sensitivity to image noise and initialization. This improvement is achieved by modifying the force that drives the curve towards the object's edges. In traditional active contours, this force is derived from the gradient vectors of the image at C(s) and is expressed as a function of the form F(s)N, where N is the normal to curve at points [17]. This results in a speed of movement of κ F(s)N, where κ represents the curvature of the curve. However, in the presence of image noise, the gradient vectors can become erratic, leading the curve in unwanted directions.

This study aimed to develop a new model for segmenting melanoma lesions from skin images. The model is based on enhancing a specific set of algorithms that have already shown some success in this task [18]. These algorithms are known as GVFACs, which represent a more advanced form of active contours. The phase of active contour models is defined over a curve C(s) with the object model represented by the zero-level set of a function u(x,y). The curve moves towards the object boundary by evolving u to minimize an energy functional.

1.3 Scope

Considering the scope of this paper, it is crucial to recognize the potential impact such a system could have on the medical industry. Early detection of skin melanoma could save thousands of lives and significantly reduce the costs and burdens currently placed on the healthcare system for treating advanced skin cancer. A non-invasive, cost-effective early detection method could also lower the expenses associated with the diagnosis and treatment of patients [19]. Additionally, a reliable method for early detection of skin melanoma can provide peace of mind to individuals uncertain about whether a particular skin lesion is cancerous, thereby improving the quality of life for those at risk [20]. Given these considerations, a dependable method for the early detection of skin melanoma is highly desirable.

This paper thoroughly examines the perception of skin melanoma, the necessity of early-stage detection and recent advancements in hardware. We believe this is a critical first step towards utilizing modern machine vision algorithms for skin cancer detection, which requires a high degree of accuracy and reliability to be feasible. We also believe that recent advancements in machine vision and related algorithms have laid a foundation to make this goal achievable [21]. This research paper not only demonstrates progress towards this objective but also opens up numerous possibilities for the cost-effective and efficient early detection of skin melanoma.

2. Methodology

The second part of this project involves algorithm development. Before creating an algorithm, several key factors must be considered. First, we need to thoroughly understand the disease and acquire domain knowledge to avoid misconceptions during development. Therefore, it is essential to review prior research on the disease to be diagnosed. This ensures we do not replicate existing work and provides a reference for comparing obtained results. The final and most critical step is to

determine the characteristics of the data. By understanding these characteristics, we can select an appropriate algorithm for the data [22]. The primary goal is to develop a GVF-based algorithm to segment lesions, which will later evolve into a metaheuristic-based algorithm. The GVF is chosen for its flexible boundary, controlled by setting an external force. However, a major challenge is that GVF often gets stuck at weak edges, resulting in nonconvex boundaries after segmentation. To address this issue [23,24], enhancements such as adaptive external forces or the integration of prior knowledge can optimize the outcome.

Many metaheuristic techniques, such as simulated annealing, genetic algorithms, fuzzy logic and artificial immune systems, can serve as optimization methods for GVF segmentation. The algorithm will be developed using MATLAB, incorporating a user-friendly GUI [25].

Data collection is the initial stage of the diagnostic system and it is the most critical, as the quality of the data directly affects the accuracy, speed and reliability of the results. Melanoma images will be gathered from the National University Hospital of Singapore (NUHS) and the Department of Dermatology at the National Skin Centre (NSC), both of which have announced the availability of online clinical and dermoscopic image sets [26]. These images have been obtained from skin lesions that were histopathologically confirmed after diagnosis.

These images included both malignant and benign melanoma cases. Dermoscopy, a contact-based, non-invasive microscopic technique, was used to examine the colour and microstructure of the lesions. Dermoscopic analysis of skin lesions has been shown to enhance the diagnosis of melanoma and reduce the number of unnecessary excisions of benign lesions. Utilizing a combination of clinical and dermoscopic images is expected to improve the sensitivity, specificity and overall accuracy of melanoma detection. Therefore, this research will benefit from the integration of both image types [27]. It is crucial that the skin lesions are clearly visible in the images, as illustrated in Figure 1. These images will be stored in a matrix format, with data collected on the lesion type (malignant or benign). The data will then undergo preprocessing before advancing to the next stage.

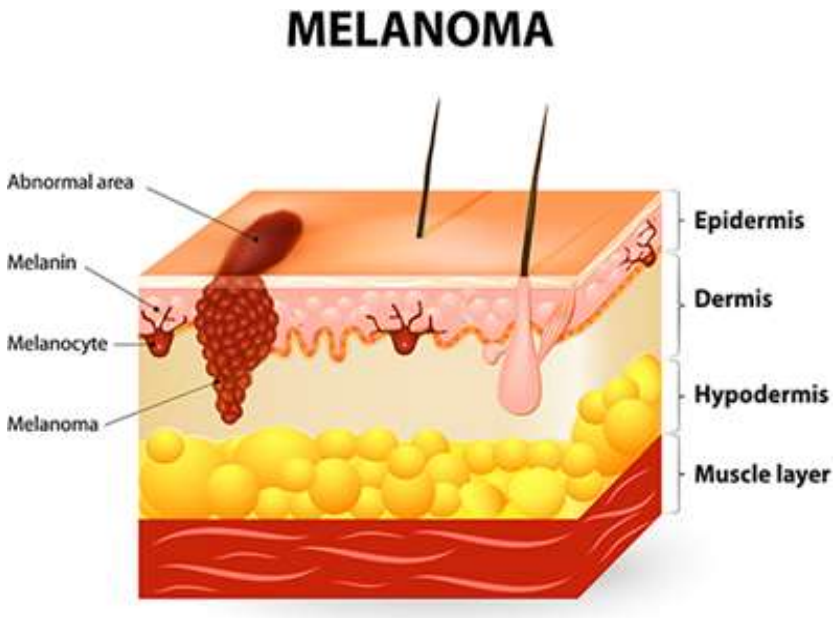

Fig. 1. Malignant melanoma

2.1 Data Collection

Next, we can assume that u (x, y), where (x, y) is a point inside or on the boundary of R, is a function that separates R by assigning a value of 1 to the area in-side R and 0 to the area outside R.

This function can be constructed to link with the Meta-GVF algorithm by using an initial estimated function u (x, y) that has the properties of R. The initial estimated function u (x, y) can be derived from the rough boundary image and labelled u0(x, y). Then, u (x, y) can be implemented to have the same properties as R. A simple way to achieve this, as shown in the algorithm, is by using a level set function, denoted as ϕ (x, y, t), where (x, y) is a point in an image and t is a real number [28].

A picture of a typical skin melanoma image is used, along with the marked diagnosis from a dermatologist. The image has a size of 8 bits for grayscale and 1296 x 864 pixels [29]. It consists of the normal components x and y, as well as the vector X. In this case, (x, y) represents the coordinates of the boundary points and X represents the number of boundary pixels. To simplify the processing, as shown in Figure 2, only (x, y) and the image are used because they have in-variant properties concerning the rotation of the boundary points. A region R is enclosed with a con-tour and filled with the image boundary to facilitate processing and obtain the Euclidean distance data [30].

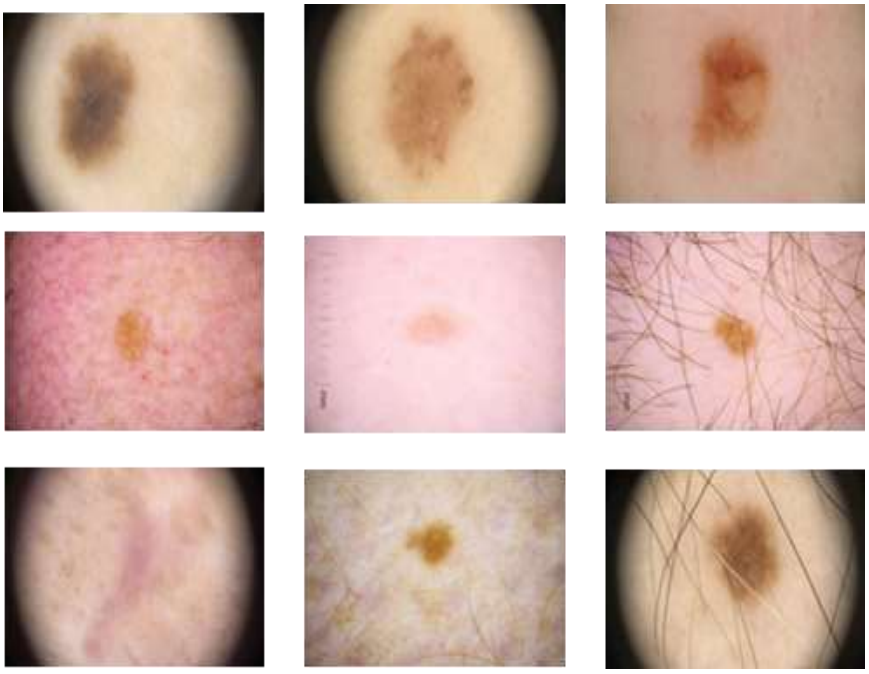

Fig. 2. Dataset sample

2.2 Algorithm Development

A preliminary step in algorithm development involved constructing several parameterized edge models. To calculate edge strength and significance, the Canny edge detector was applied to the image, with edge points parameterized based on local geometric characteristics [31]. These parameterized edges are 2D points located at ridges, valleys or inflection points of potential surface contours. The parameterization space is a 7-dimensional space that includes the 3D position of the point, the tangent and the surface normal to the underlying surface contour.

An edge point model was developed under the assumption that a true edge direction defines the steepest contrast change path across an edge and that the surface normal aligns with the gradient of the image across the edge, perpendicular to the true edge direction. Let v(x) be a vector spanning from one side of the potential surface contour to the other and let X (s, n) be a parameterization of a specific edge point. An energy function E(v) can be formulated as the dot product of the vector v and the difference between the parameterized edge point and the vector, where X denotes the vector magnitude [32]. The edge point direction is then defined as the minimum of E. This model was

tested on two sets of simulated data with known surface normal and edge strengths, yielding promising results.

2.3 Evaluation Metrics

When diagnosing melanoma, sensitivity and specificity are crucial because clinical decisions are based on these metrics. There is an inverse relationship between sensitivity and specificity, where adjusting the decision threshold to favour one metric typically reduces the other. A common way to visualize diagnostic test performance is through a receiver operating characteristic (ROC) curve, which plots the true positive rate (sensitivity) against the false positive rate (1-specificity). An area under the ROC curve (AUC) of 1 represents a perfect test, while an AUC of 0.5 indicates a test with no diagnostic value [33]. The ROC curve is useful for comparing tests and determining the optimal cut-off point for diagnostic decisions.

Another valuable tool is the precision-recall (PR) plot, which is particularly relevant for imbalanced datasets. The PR plot graphs precision (positive predictive value) against recall (sensitivity) and is helpful when the positive class is of primary interest, as it directly represents these metrics. Both the ROC and PR plots compare test outcomes to known truths. While these tools are effective for research, a single summary measure is often needed for practical application. This can be obtained by selecting a specific point on the ROC curve and calculating the Euclidean distance from the point (1,1) on the ROC plot [34]. This measure, known as the Youden index, is derived from the square root of the sum of the squares of sensitivity and specificity minus one. Additionally, a pseudo-receiver operating characteristic (PROC) curve can be generated by substituting various threshold values into a logistic model and plotting the resulting sensitivity and specificity. This helps illustrate how different thresholds impact diagnostic accuracy.

Finally, the confusion matrix is a square matrix that displays actual values in the columns and the model's predicted values in the rows or *vice versa* [33]:

i. TP: True Positive: The actual value was positive and the model predicted a positive value.
ii. FP: False Positive: Your prediction is optimistic and it is false. (Also known as the Type 1 error).
iii. FN: False Negative: Your prediction is pessimistic and the result it is also false. (Also known as the Type 2 error).
iv. TN: True Negative: The actual value was negative and the model predicted a negative value.

In the Eq. (1) to Eq. (4) below, the efficiency and accuracy of the model are calculated:

$$\text{Accuracy} = \frac{TP+TN}{TP+FP+TN+FN} \quad (1)$$

$$Fscore = \frac{2*TP}{2*TP+FN+fp} \quad (2)$$

$$\text{Precision} = \frac{TP}{TP+FP} \quad (3)$$

$$\text{Recall} = \frac{TP}{TP+FN} \quad (4)$$

2.4 Statistical Analysis

The second method of analysis involves comparing the predicted outputs to the true outputs of the data. Since our data are binary (benign/malignant) and the algorithm is linear, this comparison is straightforward. The results are often summarized using a misclassification table. Both methods are versatile and can provide valuable insights into the classifier's performance.

The first evaluation method used was ROC analysis. The ROC curve is a graphical technique for assessing the performance of a classifier. A test with known results (e.g., comparing the classification of a case by our algorithm to the classification by a dermatologist) produces a sensitivity/specificity pair [33]. A classifier is considered superior if it provides greater sensitivity for the same specificity, ideally reaching the top left-hand corner of the graph. This performance can be summarized by a single number: the area under the ROC curve AUC. A perfect classifier would have an AUC of 1, while a random classifier would have an AUC of 0.5. This technique is particularly useful when balancing the trade-offs between false positives and false negatives, as it offers the flexibility to decide what is acceptable [33].

The statistical analysis involved comparing the outputs of previous models with those of Meta-GVF using various evaluation metrics. These metrics offer quick insights into the model's accuracy, the types of errors made and the confidence level of the predictions. This overall summary is essential for comparing different models and determining their predictive capabilities.

In our research, we used a cross-validation method that omits one case at a time from the full dataset. This method involves fitting the model to all cases except the one to be classified [34] and then making a prediction. A confusion matrix is subsequently formed to gather detailed statistics. This process was repeated with a training/testing split of 90% of the data, yielding equally promising results, as illustrated in Figure 3.

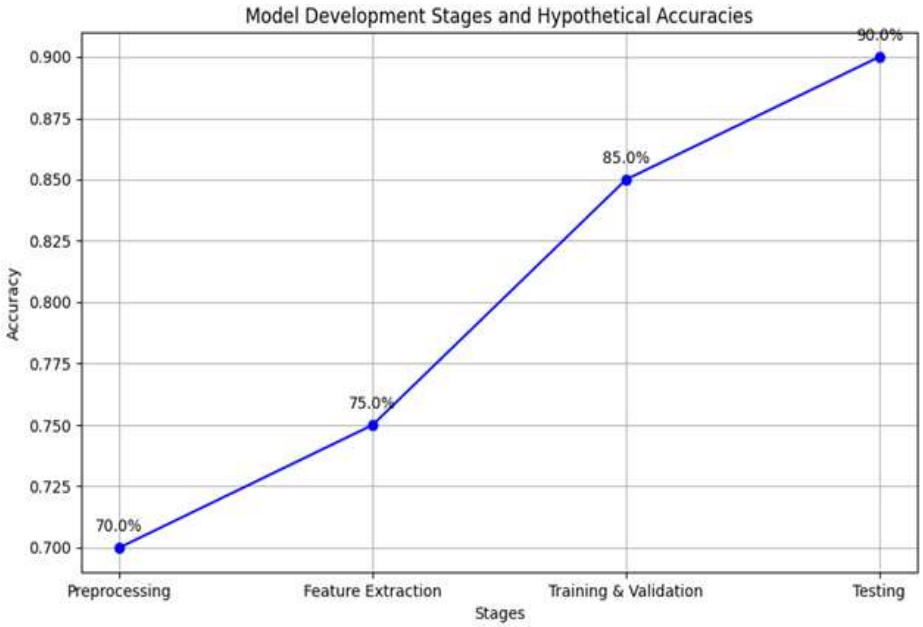

Fig. 3. Model development stages

3. Results

Both the improved and original versions of the Meta-GVF snake algorithm were tested on a set of 120 images representing 40 patients, each with a lesion verified as malignant melanoma. The

lesions were marked by three experts. These images are the same ones used in the original GVF snake paper. To ensure consistency and the validity of results, all parameters for the snake were kept constant, as in the original study. Several similarity and visualization measures were employed to quantify the algorithm's performance. The similarity between the segmented boundary and the ground truth of the lesion was assessed using a method adapted from the kidney segmentation paper. This approach involved calculating the average distance of the segmented boundary from the ground truth, with false positive sections and boundary indentations penalized accordingly. Visualization of snake convergence allowed for visual analysis of the algorithm's performance, providing insights into the challenges encountered with each method.

The Meta-GVF algorithm has shown promising results in the automatic detection of skin lesion boundaries. This method, which uses active contouring driven by forces derived from localized edge information, has proven successful, as illustrated in Figure 4.

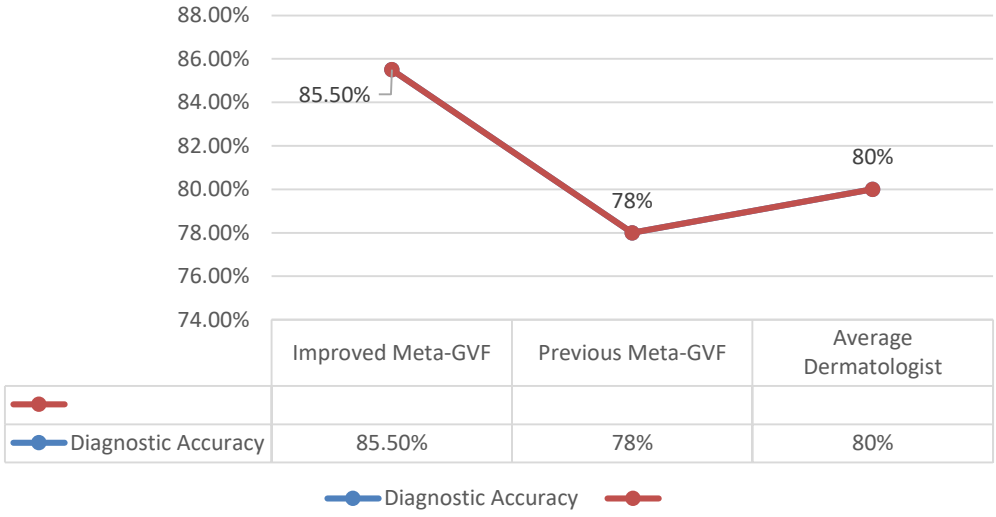

Fig. 4. Summary of results

Also, Figures 6 and 7 compare the performance of the unimproved and improved Meta-GVF algorithms, respectively. In both cases, the snake began well within the actual lesion but did not converge to the correct location. In Figure 6, representing the unimproved algorithm, the snake converged to a minor gradient ridge in the image, resulting in the under-segmentation of half of the lesion. Additionally, the snake leaked due to weak boundary constraints, drifting left towards another lesion in the image. In contrast, Figure 7, which shows the improved algorithm, demonstrates no leaked edges, with the snake converging to the correct location. This pattern was common with the unimproved algorithm; however, the improved algorithm generally converged more effectively to the minimum energy position across all image cases. This improvement contributed to the removal of line integration bias. The visualizations confirmed that the improved algorithm achieved better convergence compared to the other methods, as reflected in the significant enhancements observed in the similarity measures of the improved method.

3.1 Performance of the Improved Meta-GVF Algorithms

The Meta-GVF algorithm represents an improvement on the original GVF algorithm by incorporating meta-parameters that enhance its ability to handle noisy images and images with weak edge data. This study employed a variation of the improved Meta-GVF algorithm throughout the

entire process to ensure project quality. The key difference between the GVF algorithm and the Meta-GVF algorithm lies in the computation of v creates the external force field. In the GVF model, this step generates force at each point along the normalized gradient, with no guarantee of stopping at weak edges. This can result in the algorithm leaking through to the opposite side of an edge point, causing the point to no longer be on the curve. As the GVF model evolves, the magnitude of the external forces increases, leading the curve to be influenced by forces away from weak edges and noisy data points, which can cause the snake to skip or miss desired features entirely.

The GVF algorithm tends to overly push the curve toward the real edge of the image. In contrast, the Meta-GVF algorithm constructs the force field by multiplying the normalized gradient by a function Ø, where the Laplacian of this function equals the gradient magnitude of Ø. The solution for v is found by performing gradient descent on the functional E(v). This method is effective in stopping at weak edges and noisy data points, as forces normal to strong edges are proportionally greater, with the force field eventually reaching zero at edge points. The improved Meta-GVF algorithm was used in place of traditional active contour routines, representing a new curve in a simpler form. The movement of the curve is dictated by its evolution toward minimizing the energy function. The improved Meta-GVF algorithm produced more consistent and meaningful results, particularly with noisy and low-quality image data. This algorithm was directly compared to the GVF algorithm, yielding similar results but with less complex and more efficient programming, as shown in Figure 5. While the improved Meta-GVF algorithm does have increased computational requirements, modern computers can handle the implementation with acceptable run times for medical image processing.

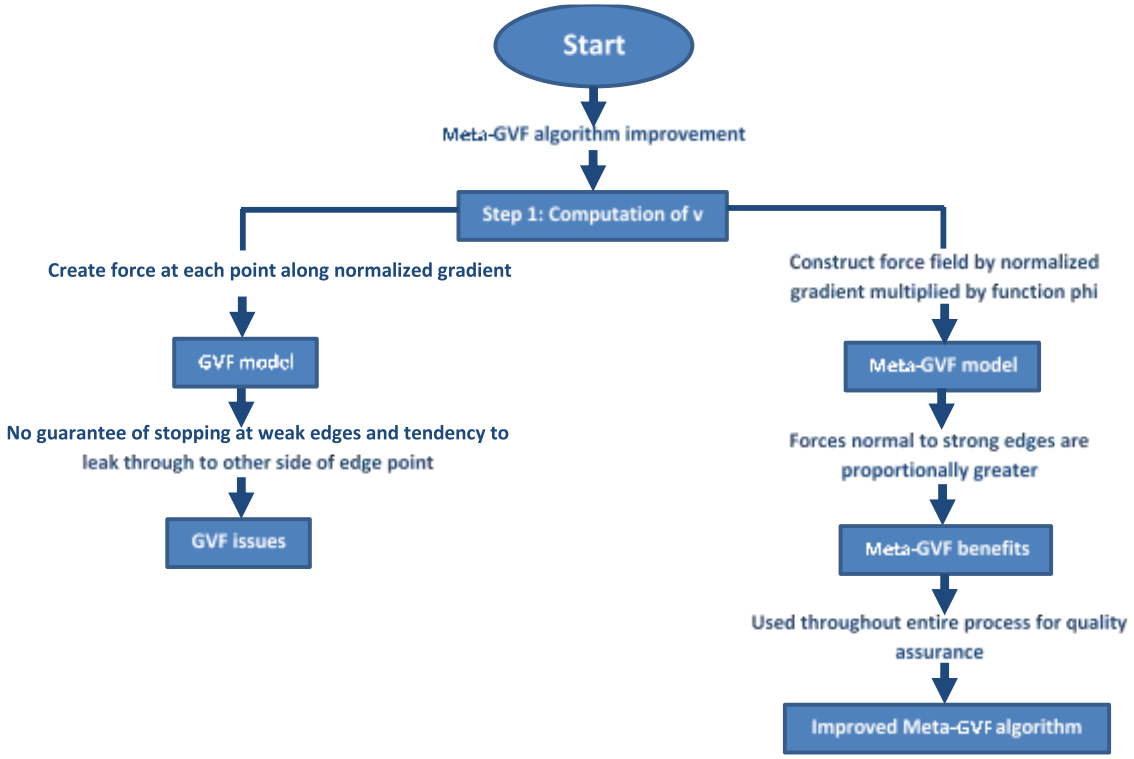

Fig. 5. A comparative flowchart of the GVF and improved Me-ta-GVF algorithm enhancements

3.2 Comparison with Existing Methods

The Hausdorff distance is a measure that represents the maximum distance from a point in one set to the nearest point in the other set. It is a consistent measure and provides a good indication of how closely the calculated boundary matches the actual boundary. Our recent algorithm yields a

Hausdorff distance of 4.96, a significant improvement over the LBF method, which has a distance of 7.00 and the GVF method, which has a distance of 8.25. In a direct comparison of boundaries, the Meta-GVF algorithm demonstrated a superior ability to adhere to grayscale changes in the image. This is crucial because most lesions are detected based on colour variations. This improvement is illustrated in Figure 5, where the paths taken by all three algorithms are overlaid on an image showing the magnitude of the edge potential force in the normal direction.

The results of the improved Meta-GVF algorithm are compared with those of the previous GVF approach and the LBF framework. The comparison demonstrates that our algorithm successfully segments the lesion and its calculated boundary outperforms those of existing methods as measured by MFT and the Hausdorff distance. We compute the MFT of the lesion boundary by dividing the distance through the path by the number of boundary pixels it travels, which is a consistent measure of boundary length. We were able to achieve MFT = 1.05, which is a near-perfect result. The LBF is considerably worse at MFT = 1.31 and our previous GVF attempt on these data had MFT = 1.21, as shown in the diagram in Figure 6.

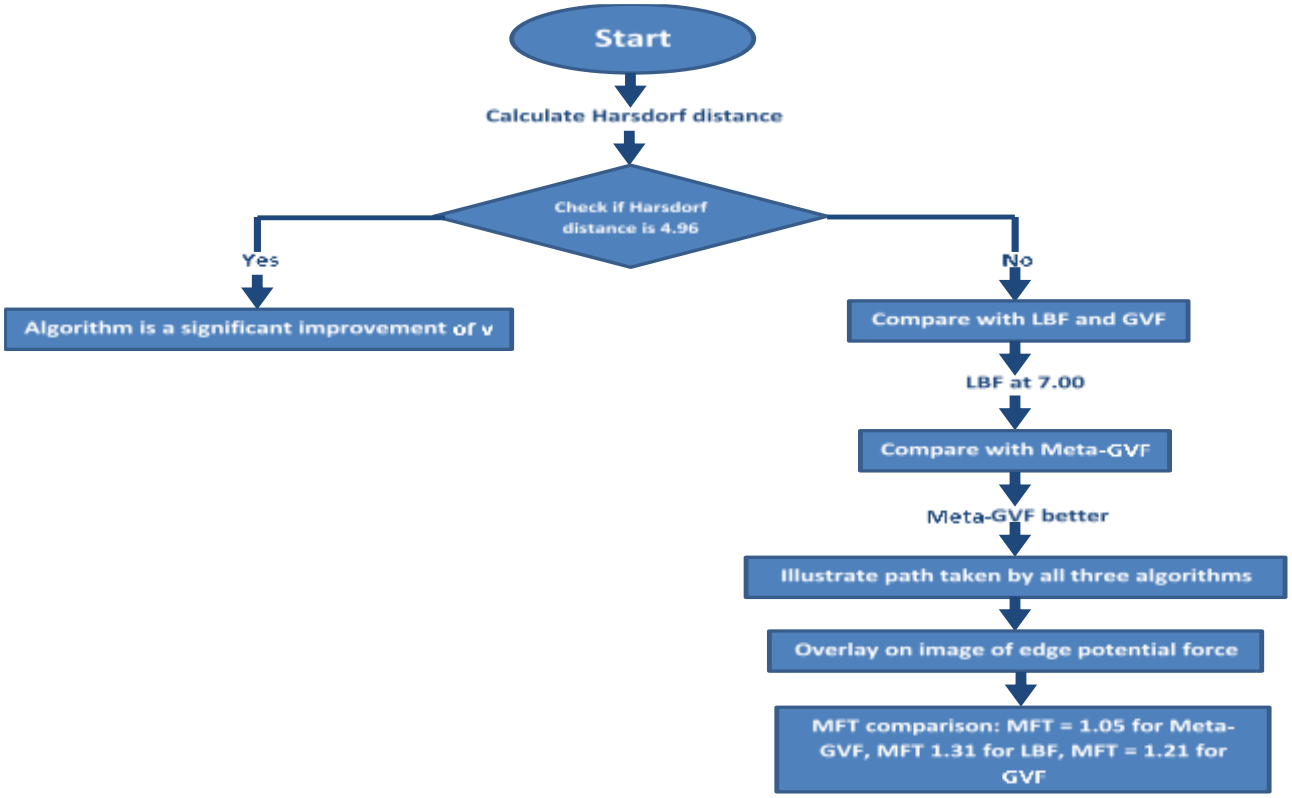

Fig. 6. Flowchart of algorithm performance evaluation and comparison based on Harsdorf distance and MFT

3.3 Clinical Implications

In this study, the globally and locally improved Meta-GVF algorithms yielded an average accuracy of 85.5%. This marks a significant improvement over our previous result of 78%. Given that the current accuracy of dermatologists in diagnosing lesions is estimated to be around 80%, the improved Meta-GVF method shows potential as a computer-assisted diagnostic tool. Notably, this can be achieved without requiring large amounts of computational power.

A trial conducted a few years ago, which compared different dermatologists' diagnostic capabilities for the same lesion, revealed that the most experienced dermatologists are not always the most accurate. In this trial, dermatologists were asked to diagnose 40 different lesions and

classify them as benign or malignant. Although 5 of the lesions were later identified as invasive malignant melanoma, some dermatologists did not diagnose any of the 40 lesions as melanoma. This outcome was partly due to some dermatologists' belief that it is better to miss a few early melanomas than to misdiagnose benign lesions as malignant. The improved accuracy of the Meta-GVF algorithm could assist dermatologists by prompting them to consider morphology when diagnosing pigmented lesions, which they may not always do, as illustrated in Figure 7 and Table 2. This could significantly reduce the number of early melanomas that are missed.

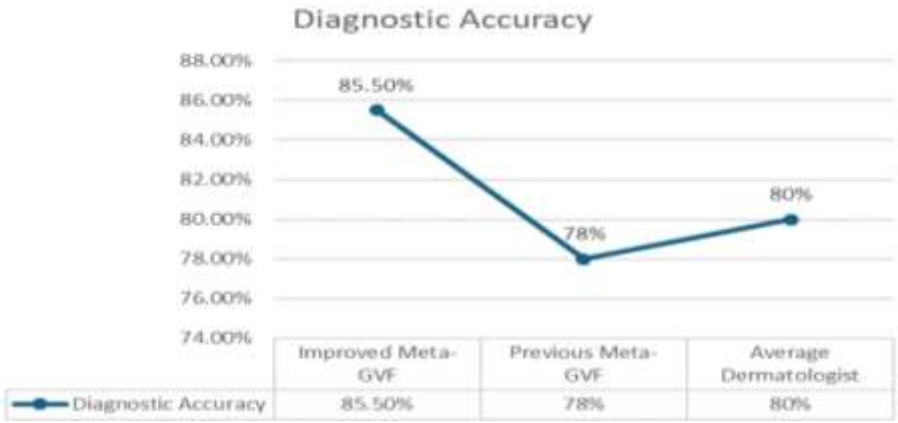

Fig. 7. Diagnostic accuracy

Table 2
Evaluation metrics for the proposed method

Accuracy	Precision	Recall	F-score
85.5	85.7	75.0	79.9

4. Conclusion

The Meta-GVF has demonstrated exceptional automatic tracking performance for boundaries in both 2D and 3D motion. Using both conventional and advanced active contour models, we have observed that the recorded boundary can often be over- or under-tracked. To achieve improvements over the current state of the art, a ground truth database is necessary, as there are currently no reliable means of extracting accurate boundary information from manually drawn boundaries.

This challenge has been addressed through shape modelling and by providing initial conditions close to the solution, which allows the contour to move toward the correct boundary. With further advancements, it may be possible to use boundary detection methods to determine the initial conditions for the Meta-GVF solution, enabling the automatic detection and diagnosis of skin abnormalities.

Given the strong tracking properties demonstrated by Meta-GVF algorithms, it would be valuable to compare and optimize these algorithms for boundary detection problems in the imaging of other physical systems, potentially leading to significant success in these areas as well. Additionally, for future research, there are several directions researchers could explore, such as integrating the proposed model with deep learning techniques to develop real-time diagnostic tools and employing cross-dataset validation to enhance model performance.

Acknowledgement
This research was not funded by any grant.

References

[1] Marchetti, Michael A., Konstantinos Liopyris, Stephen W. Dusza, Noel CF Codella, David A. Gutman, Brian Helba, Aadi Kalloo *et al.,* "Computer algorithms show potential for improving dermatologists' accuracy to diagnose cutaneous melanoma: Results of the International Skin Imaging Collaboration 2017." *Journal of the American Academy of Dermatology* 82, no. 3 (2020): 622-627. https://doi.org/10.1016/j.jaad.2019.07.016

[2] Abd-Alzhra, Arwa Sahib, and Mohammed SH Al-Tamimi. "Image compression using deep learning: methods and techniques." *Iraqi Journal of Science* (2022): 1299-1312. https://doi.org/10.24996/ijs.2022.63.3.34

[3] Al-Majeed, Shaimaa A., and Mohammed SH Al-Tamimi. "Survey Based Study: Classification of Patients with Alzheimer's Disease." *Iraqi Journal of Science* 61, no. 11 (2020). https://doi.org/10.24996/ijs.2020.61.11.31

[4] Nasir, Muhammad, Muhammad A. Khan, Muhammad Sharif, Muhammad Younus Javed, Tanzila Saba, Hashim Ali, and Junaid Tariq. "Melanoma detection and classification using computerized analysis of dermoscopic systems: a review." *Current Medical Imaging* 16, no. 7 (2020): 794-822. https://doi.org/10.2174/1573405615666191223122401

[5] Mijwil, Maad M., Omega John Unogwu, and Karan Kumar. "The role of artificial intelligence in emergency medicine: a comprehensive overview." *Mesopotamian Journal of Artificial Intelligence in Healthcare* 2023 (2023): 1-6. https://doi.org/10.58496/MJAIH/2023/001

[6] Al-Mistarehi, Abdel-Hameed, Maad M. Mijwil, Youssef Filali, Mariem Bounabi, Guma Ali, and Mostafa Abotaleb. "Artificial intelligence solutions for health 4.0: overcoming challenges and surveying applications." *Mesopotamian Journal of Artificial Intelligence in Healthcare* 2023 (2023): 15-20. https://doi.org/10.58496/MJAIH/2023/003

[7] Mohamed Ishaq.H, Hariprasath.S, Lavanya.K, Divya.B, Mahalaksmi B, and Nandhini J. "An Overview of Various Cancer Treatments of Melanoma and Its Diagnosis". *Journal of Coastal Life Medicine* 11 (1), (2023): 1404-20. https://www.jclmm.com/index.php/journal/article/view/536

[8] Jeihooni, Ali Khani, Pooyan Afzali Harsini, Gholamreza Imani, and Saeed Hamzehie. "Melanoma Epidemiology: Symptoms, Causes, and Preventions." In Melanoma-Standard of Care, Challenges, and Updates in Clinical Research. IntechOpen, 2023. https://doi.org/10.5772/intechopen.107096.

[9] Olsen, Catherine M., Nirmala Pandeya, Bruna S. Ragaini, Rachel E. Neale, and David C. Whiteman. "International patterns and trends in the incidence of melanoma and cutaneous squamous cell carcinoma, 1989–2020." *British Journal of Dermatology* 190, no. 4 (2024): 492-500. https://doi.org/10.1093/bjd/ljad425

[10] Mukherjee, Soumen, Arunabha Adhikari, and Madhusudan Roy. "Melanoma detection from lesion images using optimized features selected by metaheuristic algorithms." *International Journal of Healthcare Information Systems and Informatics (IJHISI)* 16, no. 4 (2021): 1-22. https://doi.org/10.4018/IJHISI.288542

[11] Zhang, Yiming, and Chong Wang. "SIIM-ISIC melanoma classification with DenseNet." In *2021 IEEE 2nd international conference on big data, artificial intelligence and internet of things engineering (ICBAIE)*, pp. 14-17. IEEE, 2021. https://doi.org/10.1109/ICBAIE52039.2021.9389983

[12] Dziankowska-Zaborszczyk, Elżbieta, Irena Maniecka-Bryła, and Małgorzata Pikala. "Mortality trends due to skin melanoma in Poland in the years 2000–2020." *International Journal of Environmental Research and Public Health* 19, no. 23 (2022): 16118. https://doi.org/10.3390/ijerph192316118

[13] Tahat, Majd, Belal Abuata, and Maryam Nuser. "Computer Aided Diagnosis of Melanoma Based on the ABCD Rule." *International Journal of Computing and Digital Systems* 12, no. 1 (2022): 643-652. https://doi.org/10.12785/ijcds/120152

[14] Das, Jaya Bijaya Arjun, Debahuti Mishra, Abhishek Das, Mihir Narayan Mohanty, and Archana Sarangi. "Skin cancer detection using machine learning techniques with ABCD features." In *2022 2nd Odisha International Conference on Electrical Power Engineering, Communication and Computing Technology (ODICON)*, pp. 1-6. IEEE, 2022. https://doi.org/10.1109/ODICON54453.2022.10009956

[15] Fawzy, Shimaa, Hossam El-Din Moustafa, Ehab H. AbdelHay, and Mohamed Maher Ata. "Proposed optimized active contour based approach for accurately skin lesion segmentation." *Multimedia Tools and Applications* 83, no. 2 (2024): 5745-5797. https://doi.org/10.1007/s11042-023-15436-4

[16] Al-Masni, Mohammed A., Dong-Hyun Kim, and Tae-Seong Kim. "Multiple skin lesions diagnostics via integrated deep convolutional networks for segmentation and classification." *Computer methods and programs in biomedicine* 190 (2020): 105351. https://doi.org/10.1016/j.cmpb.2020.105351

[17] Shah, Aarushi, Manan Shah, Aum Pandya, Rajat Sushra, Ratnam Sushra, Manya Mehta, Keyur Patel, and Kaushal Patel. "A comprehensive study on skin cancer detection using artificial neural network (ANN) and convolutional neural network (CNN)." *Clinical eHealth* 6 (2023): 76-84. https://doi.org/10.1016/j.ceh.2023.08.002

[18] Adegun, Adekanmi, and Serestina Viriri. "Deep learning techniques for skin lesion analysis and melanoma cancer detection: a survey of state-of-the-art." *Artificial Intelligence Review* 54, no. 2 (2021): 811-841. https://doi.org/10.1007/s10462-020-09865-y

[19] Bhatt, Harsh, Vrunda Shah, Krish Shah, Ruju Shah, and Manan Shah. "State-of-the-art machine learning techniques for melanoma skin cancer detection and classification: a comprehensive review." *Intelligent Medicine* 3, no. 03 (2023): 180-190. https://doi.org/10.1016/j.imed.2022.08.004

[20] Jovic, Dragomirka, Xue Liang, Hua Zeng, Lin Lin, Fengping Xu, and Yonglun Luo. "Single-cell RNA sequencing technologies and applications: A brief overview." *Clinical and translational medicine* 12, no. 3 (2022): e694. https://doi.org/10.1002/ctm2.694

[21] Mohd Ghani, Noor Ain Syazwani, and Abdul Kadir Jumaat. "Selective segmentation model for vector-valued images." *Journal of Information and Communication Technology* 21, no. 02 (2022): 149-173. https://doi.org/10.32890/jict2022.21.2.1

[22] Ghani, Noor Ain Syazwani Mohd, Abdul Kadir Jumaat, Rozi Mahmud, Mohd Azdi Maasar, Farizuwana Akma Zulkifle, and Aisyah Mat Jasin. "Breast abnormality boundary extraction in mammography image using variational level set and self-organizing map (SOM)." *Mathematics* 11, no. 4 (2023): 976. https://doi.org/10.3390/math11040976

[23] Moradzadeh, Arash, Sahar Zakeri, Maryam Shoaran, Behnam Mohammadi-Ivatloo, and Fazel Mohammadi. "Short-term load forecasting of microgrid via hybrid support vector regression and long short-term memory algorithms." *Sustainability* 12, no. 17 (2020): 7076. https://doi.org/10.3390/su12177076

[24] Mohan, Chakrabhavi Dhananjaya, Shobith Rangappa, S. Chandra Nayak, Ragi Jadimurthy, Lingzhi Wang, Gautam Sethi, Manoj Garg, and Kanchugarakoppal S. Rangappa. "Bacteria as a treasure house of secondary metabolites with anticancer potential." In *Seminars in cancer biology*, vol. 86, pp. 998-1013. Academic Press, 2022. https://doi.org/10.1016/j.semcancer.2021.05.006

[25] Nazzaro, Gianluca, Emanuela Passoni, Fabio Pozzessere, Carlo Alberto Maronese, and Angelo Valerio Marzano. "Dermoscopy use leads to earlier cutaneous melanoma diagnosis in terms of invasiveness and size? A single-center, retrospective experience." *Journal of Clinical Medicine* 11, no. 16 (2022): 4912. https://doi.org/10.3390/jcm11164912

[26] Shaqfa, Mahmoud, Gary PT Choi, Guillaume Anciaux, and Katrin Beyer. "Disk harmonics for analysing curved and flat self-affine rough surfaces and the topological reconstruction of open surfaces." *Journal of Computational Physics* 522 (2025): 113578. https://doi.org/10.1016/j.jcp.2024.113578

[27] Alam, Bashir, and Mansaf Alam, eds. *Intelligent Data Analytics, IoT, and Blockchain*. CRC Press, 2023. https://doi.org/10.1201/9781003371380

[28] Ge, Pengqiang, Yiyang Chen, Guina Wang, and Guirong Weng. "An active contour model based on Jeffreys divergence and clustering technology for image segmentation." *Journal of Visual Communication and Image Representation* 99 (2024): 104069. https://doi.org/10.1016/j.jvcir.2024.104069

[29] Naik, Gunjan, Shubhangi Kelkar, Bhushan Garware, and Aditya Abhyankar. "Adaptive kernel-based active contour." *International Journal of Computational Vision and Robotics* 13, no. 2 (2023): 202-218. https://doi.org/10.1504/IJCVR.2023.129439

[30] Bozorgmehri, Babak, Leonid P. Obrezkov, Ajay B. Harish, Aki Mikkola, and Marko K. Matikainen. "A contact description for continuum beams with deformable arbitrary cross-section." *Finite Elements in Analysis and Design* 214 (2023): 103863. https://doi.org/10.1016/j.finel.2022.103863

[31] Nahm, Francis Sahngun. "Receiver operating characteristic curve: overview and practical use for clinicians." *Korean journal of anesthesiology* 75, no. 1 (2022): 25-36. https://doi.org/10.4097/kja.21209

[32] Pratiwi, Heny, Agus Perdana Windarto, S. Susliansyah, Ririn Restu Aria, Susi Susilowati, Luci Kanti Rahayu, Yuni Fitriani, Agustiena Merdekawati, and Indra Riyana Rahadjeng. "Sigmoid activation function in selecting the best model of artificial neural networks." In *Journal of Physics: Conference Series*, vol. 1471, no. 1, p. 012010. IOP Publishing, 2020. https://doi.org/10.1088/1742-6596/1471/1/012010

[33] Jaskowiak, Pablo A., Ivan G. Costa, and Ricardo JGB Campello. "The area under the ROC curve as a measure of clustering quality." *Data Mining and Knowledge Discovery* 36, no. 3 (2022): 1219-1245. https://doi.org/10.1007/s10618-022-00829-0

[34] Yates, Luke A., Zach Aandahl, Shane A. Richards, and Barry W. Brook. "Cross validation for model selection: a review with examples from ecology." *Ecological Monographs* 93, no. 1 (2023): e1557. https://doi.org/10.1002/ecm.1557